Characterization of Mechanical Properties and Residual Stresses for Ni-Co Thin Films

Joong-Hyok Ahn[1,a], Hong-Yeol Bae[1,b], Yun-Jae Kim[1,c] and Jun-Hyub Park[2,d]

[1]Mechanical Engineering, Korea University, Seoul, Korea

[2]Mechatronics Engineering, Tongmyung University, Busan, Korea

[a]hyok@korea.ac.kr, [b]ollier80@korea.ac.kr, [c]kimy0308@korea.ac.kr, [d]jhyubpark@korea.com

Keywords: Elastic property, Ni-Co thin film, Plastic property, Residual stress

Abstract. The present work characterizes mechanical (elastic and plastic) properties and residual stresses of a Ni-Co thin film having 10μm thickness. Mechanical properties are obtained from direct-tension testing together with elastic finite element analysis. Membrane and bending components of residual stresses are measured using micro-cantilever and T-structure tests, respectively.

Introduction

Measurement of residual stresses in thin films is quite important, as their effect on mechanical integrity of micro-electrical-mechanical components could be significant. A number of measurement methods are available [1-7], but a majority of methods deal with measuring averaged residual stresses, rather than thickness-variation of residual stresses in thin films. Although such thickness variation could be often insignificant due to the fact that the thickness is very small, residual stresses can vary along the thickness of thin films. Measuring thickness variations of residual stresses, however, are not straightforward. A sectioning method can be applied (see for instance Ref. [7]), but can be quite tedious. In this respect, a simple method to measure thickness variations is desirable.

In designing (macroscopic) structures, a stresses categorization process from stresses in the thickness direction is popularly employed [8-10]. In the stresses categorization process, stresses in the thickness direction are decomposed into the primary, secondary and peak stresses. Primary stresses are ones resulting mechanical loads and dead weights. Secondary stresses include thermal and residual stresses. Both primary and secondary stresses are typically idealized as a sum of (constant) membrane and (linear) bending stress components. Remaining stresses are classified as the peak stress, which relaxes quickly with plastic deformation by definition. A message that can be learnt from conventional stresses categorization process is that determination of membrane and bending components of residual stresses would be sufficient from mechanical integrity point of view.

This paper presents measurement of residual stresses in Ni-Co thin films. A linearly-varying residual stress across the film thickness is assumed. To measure its bending and membrane components, cantilever beam and T-structure beam specimens are used, respectively.

Experiments

Material and Specimen Fabrication A NiCo thin film is recently widely used for MEMS devices using LIGA processes. Fabrication processes of NiCo thin film specimens are schematically shown in Fig. 1. For tensile test, conventional “dogbone” tensile test specimens were fabricated. Furthermore, for residual stress analysis, specimens of T-type structure and cantilever beams (which will be discussed later in this paper) with various dimensions were also fabricated. A single-side

polished 6-inch silicon wafer with (100) surface was used as a substrate. For electro-plating of NiCo, a 100 nm thick Al was deposited by sputtering process as a seed layer (Fig. 1a). The Al film on the front-side also plays a role as a hard mask when the substrate would be etched by deep reactive ion etching. The photo resist (PR) was coated and then was patterned by photolithography (Fig. 1b). The NiCo film to be tested was plated by electro-plating process (Fig. 1c) and then the NiCo film of 10μm thickness was polished by chemical-mechanical polishing process (Fig. 1d). The photo resist layer was then removed, as shown in Fig. 1e. The open area below the test film was patterned on the backside and the silicon substrate was dry-etched by the deep reactive ion etching process until reaching Al layer and then the seed layer was etched by wet etching process for making a freely standing specimen without damaging the NiCo film, as shown in Fig. 1f. The fabricated specimen is shown in Fig. 1g. Each specimen was diced by laser.

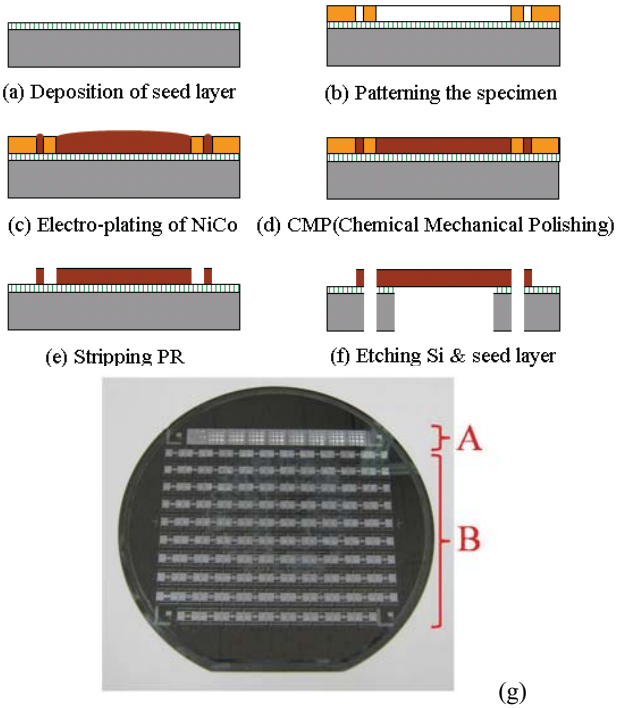

Fig. 1. Fabrication processes for manufacturing NiCo thin film specimens, and the wafer with specimens, indicating specimens for tensile tests ("A") and residual stress measurements ("B").

Tensile Tests To measure residual stresses, elastic moduli of thin films should be firstly determined. Although there are several methods to measure elastic moduli of thin films [11-20], the present work utilized direct tensile tests using the microtensile-testing machine developed by authors [21,22]. The testing machine is equipped with a load-cell (for measuring load) and a capacitance sensor (for measuring displacement between grips). More detailed descriptions for the micro-tensile testing machine, used in the present work, can be found in Refs. [21,22].

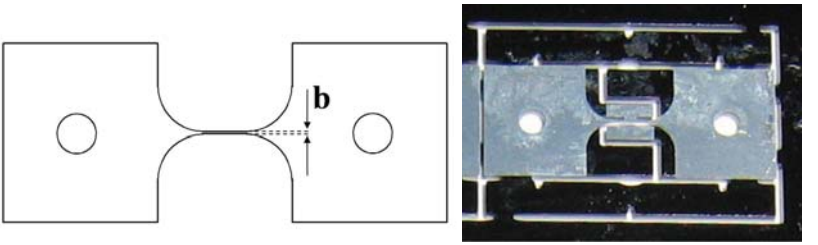

Fig. 2. Micro-tensile test specimens: schematic illustration and picture.

The authors also proposed a new specimen for tensile and fatigue tests of thin films, which is schematically shown in Fig. 2 [22]. The thickness and width of specimens were fixed to t=10μm and b=100μm, respectively. The propsoed specimen has several interesting features. Firstly the specimen can be easily mounted on the tensile tester using pins through two holes (850μm diameter) in the specimen, and thus bonding is not necessary. Secondly, to easily extract the specimen from the wafer without damaging the specimen, it is surrounded by side-support strips (made in a fabrication stage). Finally, as shown in Fig. 2, structures are also connected with grip ends of specimen to protect sudden fracture of the test film due to possibly high residual stresses in brittle passivation layers such as SiO_2 or Si_3N_4.

Cantilever Beam Tests Simple cantilever beams were fabricated to measure residual stresses, as shown in Fig. 3. Although the thickness was fixed to t=10 μm, beams with different in-plane dimensions were fabricated. For the length L, two different values, L=300 and 700 (μm), were chosen, whereas those of the width b were systematically varied from b=10μm to b=100 μm.

In the presence of residual stresses, cantilever beams will deflect, as schematically shown in Fig. 3. To measure end deflections of cantilever beams, 3-D imaging surface structure analyzer (the NT-2000 made by Veeco, USA) was used, as shown in Fig. 4a. Resolutions of this equipment are 3nm using the vertical scanning mode (used in this work), but can be 1 Å using the phase-shifting mode. Figure 4b illustrates measured imaging surfaces of cantilever beams with L=700μm and b=80, 90 and 100μm, from which end deflections can be measured. Resulting end deflections δ are summarized in Fig. 5. For specimens with L=300 μm, values of δ range from ~2.1 μm to ~2.5 μm, whereas for L=700μm, from ~11.5 μm to ~14.2 μm. Figures also include mean values and standard deviations of experimental values.

T-Structure Beam Tests To measure residual stresses, another type of specimens was also fabricated, so-called the T-structure beam, proposed in Ref. [3], as shown in Fig. 6. This specimen has four dimensions, t, L, L_s and W (Fig. 7a). With the fixed thickness (t=10mm), specimens with different in-plane dimensions were fabricated: W=40, 100μm; L_s=200, 600, 1000, 1400, 1800 mm;

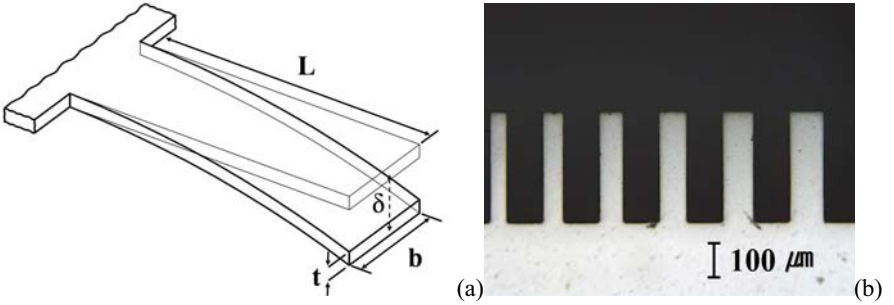

(a) (b)

Fig. 3. Cantilever beam specimens: (a) schematic illustration and (b) picture.

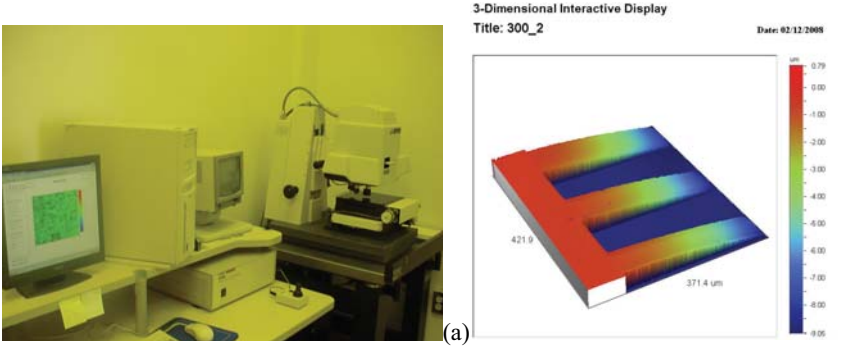

(a) (b)

Fig. 4. (a) Three-dimensional (3-D) imaging surface structure analyzer, and (b) typical 3-D imaging surfaces of cantilever beams.

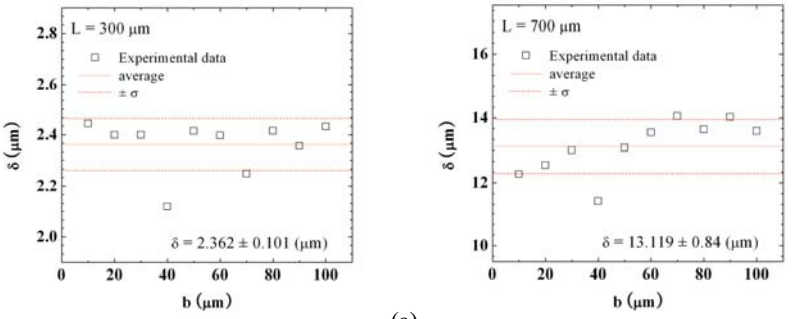

(a) (b)

Fig. 5. Typical experimental results of end deflections from cantilever beam tests: (a) L=300 μm and (b) L=700 μm.

and L=500, 1000, 1500, 2000mm. Figure 7a shows typically measured imaging surfaces of T-structure beams using 3-D imaging surface structure analyzer (NT-2000). For T-structure beams, the lateral deflection δ needs to be measured, as schematically depicted in Fig. 6a. In tests, however, it was often found that symmetry was not maintained. In this respect, to measure δ, four lengths were measured (see A_1, A_2, B_1 and B_2 in Fig. 7a), from which average values of δ were determined. Resulting lateral deflections are summarized in Fig. 7b. It can be seen that experimental results depend on L_s, but not on L and W. Furthermore experimental data show much less scatter, compared to cantilever beam tests. Values of δ vary from ~3μm to ~6 μm for L_s ranging from 600 μm to 1400 μm.

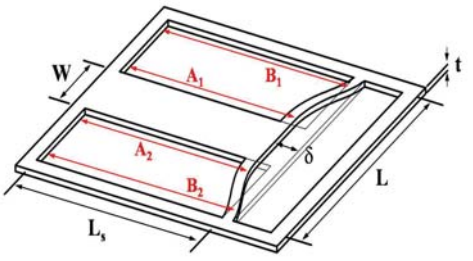

(a) (b)

Fig. 6. (a) Schematic illustration and (b) picture for T-structure beams.

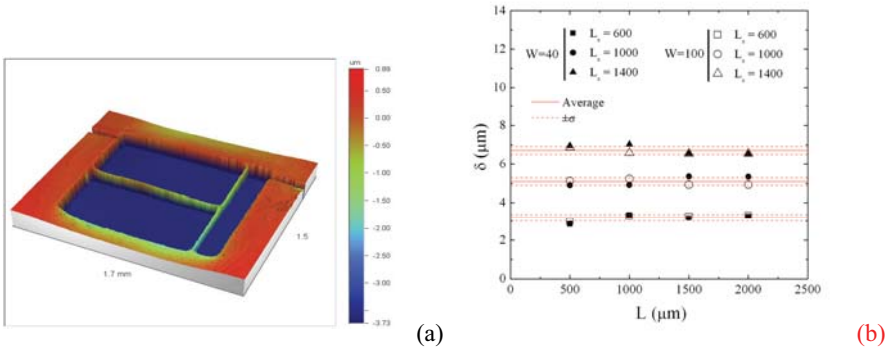

(a) (b)

Fig. 7. (a) Three-dimensional imaging surfaces of T-structure beams with W=40μm, h=20μm, L_s=1000μm and L=1000μm and (b) typical experimental results of deflections from T-structure beam tests.

Analysis and Results

Tensile Test and Elastic Modulus From tensile tests, elastic and plastic properties of the film are measured, such as elastic modulus, yield strength and tensile strength. The (engineering) tensile strength can be easily determined from experimentally-measured maximum load divided by initial cross-sectional areas. However, determination of elastic modulus and yield strength is not straightforward. It is because the tensile tester used in the present test has a capacitance displacement sensor, measuring the change of distance between grips (the total displacement). To introduce the concept of gage length, elastic FE analysis is performed using general-purpose finite element program ABAQUS [23]. Note that the present tensile specimen has a total length of 1500 μm, and a "fictitious" gauge length is set to be 300 μm. From the elastic FE analysis, the displacement ratio R can be calculated, defined by the displacement of the gauge length to the total displacement. This ratio is applied to correct initial parts of load-displacement curves and thus to determine (engineering) stress-strain data in low strain ranges. Typical processed results are shown in Fig. 8a. As the value of R is based on the elastic analysis, the correction procedure is valid only for low strain ranges, as shown in Fig. 8a. From such results, elastic modulus E and the yield strength $\sigma_{0.2}$ (defined by the 0.2% plastic strain) can be estimated, as shown in Fig. 8a. Estimated values of Young's modulus are shown in Fig. 12b, which range from E=155GPa to E=173GPa. Statistical analysis provides the average value of 163GPa with a standard deviation of 10.8GPa. Values of measured yield strengths, on the other hand, range from 1,717MPa to 1,773MPa, whereas those of tensile strengths from 1,851 MPa to 2,446 MPa.

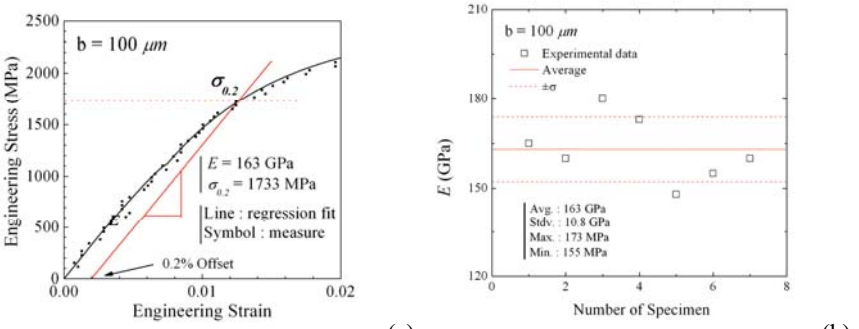

(a) (b)

Fig. 8. (a) Typical stress-strain curve, and (b) resulting values of Young's modulus for the NiCo thin film.

Micro-Cantilever Tests and Bending Residual Stresses For a cantilever beam (under plane strain condition), standard elastic analysis provides the end deflection in terms of the out-fibre bending stress σ_b:

$$\delta \cdot \frac{t}{L^2} = \frac{\sigma_b}{E}(1-\nu^2) \tag{1}$$

where ν denotes Poisson's ratio. From this equation, the out-fibre bending stress σ_b can be estimated, and results are shown in Fig. 9a. In Fig. 9a, symbols indicate estimated values of the bending residual stress σ_b using the average E value, E=163GPa. Error bars indicate variations of σ_b due to one standard variation of E. Estimated values of the bending residual stress σ_b range from ~40MPa to ~55MPa. Statistical analysis gives the average value of 47.5MPa with a standard deviation of 3.33MPa. Note that the estimated average value of σ_b=47.5MPa is quite small, compared to the yield strength ($\sigma_{0.2}$=~1700MPa).

T-Structure Tests and Membrane Residual Stresses For the T-structure beam, the membrane residual stress σ_m is related to the lateral deflection by [3]

$$\frac{\sigma_m}{E} = \delta\left(\frac{1}{L_s} + \frac{16h^3}{W\left[L^3 - W^2L + \left(W^3/2\right)\right]}\right) \tag{2}$$

Note that the right hand side of Eq. (2) consists of two terms. The first term is a function of L_s, and the second one of L, W and h. It is found that, for specimen geometries considered in the present work, the first term dominates, and the ratio of the second term to the first one is within 0.05%. Thus Eq. (2) can be simplified as

$$\frac{\sigma_m}{E} = \frac{\delta}{L_s} \tag{3}$$

Using this equation, the membrane residual stress can be estimated and results are shown in Fig. 9b. Symbols indicate estimated values of σ_m using the average E value, whereas error bars show variations due to one standard variation of E. Estimated values of the bending residual stress σ_m range from ~800MPa to ~870MPa. Statistical analysis gives the average value of 825.3MPa with a

standard deviation of 50.1MPa. Note that such σ_m values are about half of the yield strength ($\sigma_{0.2}$=~1700MPa).

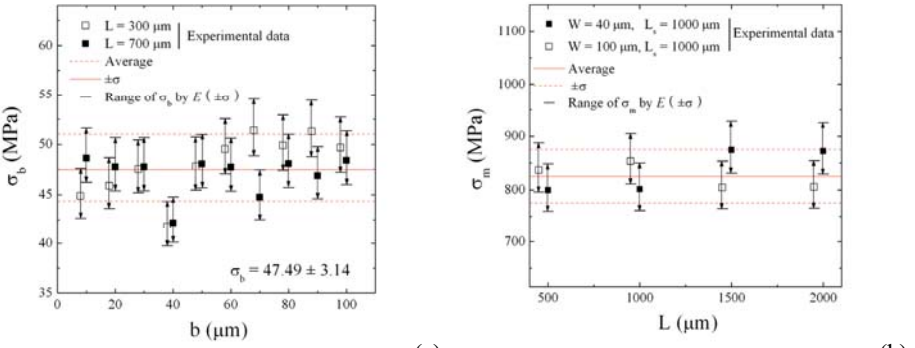

(a) (b)

Fig. 9. Estimated residual stresses in Ni-Co thin films: (a) bending component, and (b) membrane component.

Conclusions

This paper measures tensile (elastic and plastic) properties and residual stresses of a Ni-Co thin film with 10μm thickness. Mechanical properties are obtained from direct-tension testing, proposed by the authors, together with elastic finite element analysis. For residual stresses, a linearly-varying residual stress across the film thickness is assumed. To measure its bending and membrane components, cantilever beam and T-structure beam specimens are used, respectively. Estimated values of Young's modulus, yield strengths and tensile strengths range from E=155GPa to E=173GPa, from 1,717MPa to 1,773MPa, and from 1,851 MPa to 2,446 MPa, respectively. For residual stresses, estimated bending components range from ~40MPa to ~55MPa. Membrane components, on the other hand, range from ~800MPa to ~870MPa, which are about 20 times larger than bending components.

References

[1] Stoney GG (1909) Proceeding of Royal Society London A 82, 172-175.

[2] Allen MG, Mehregany M, Howe, and Senturia SD (1987) Applied Physics Letters, 51, 241-243.

[3] Mehregany M, Howe RT, Senturia SD (1987) Journal of Applied Physics, 62(9), 3579-3584.

[4] Guckel H, Burns D, Rutigliano C, Lovell E and Choi B (1992) Journal of Micromech. Microeng. 2, 86-95.

[5] Wricson F, Greek S, Soderkvist J and Schweitz J-A. (1997) Journal of Micromech. Microeng. 7, 30-36.

[6] Bhushan B (2004) Handbook of Nanotechnology, Chapter 34. Mechanical properties of micromachined structures. Springer

[7] Yang EH and Yang SS (1996) Sensors and Actuators A54, 684-689

[8] ASME Boiler and Pressure Vessel Code Section III, Section XI (1992).

[9] Penny, R. K. and Marriot, D. L. Design for Creep, 1995 (Chapman & Hall).

[10] JL Hechmer and GL Hollinger, 3D stress criteria guidelines for application, Welding Research Council Bulletin, 1998, New York.

[11] E. I. Bromley, J. N. Randall, D. C. Flanders and R. W. Mountain, J. Vac. Sci. Technol. B 1 (4) (1983) pp. 1364-1366.

[12] D. A. Hardwick, Thin Solid Film 154 (1987) pp. 109-124.

[13] Nix W. (1989) Mechanical properties of thin films. Metallurgical Transcations A 20, 2217-2245.

[14] S. Johansson, J. A. Schweitz, L. Tenez, and J. Tiren, J. Appl. Phys. 62 (10) (1988) pp. 4799-4803.

[15] K. Komai, K. Minoshima, H. Tawara, S. Inoue and K. Sunako, Trans. Jpn. Sco., Mech. Eng. A 60-569 (1994) pp. 52-58.

[16] Sharpe WN Jr, Yuan B, Edwards RL (1997) J Microelectromechanical Systems, 6, 193-199.

[17] V. T. Srikar and S. M. Spearing, Experimental Mechanics Vol. 43, No. 3, (2003), pp. 238-247.

[18] T. Connolley, P. E. Mchugh and M. Bruzzi, Fatigue Fracture Engineering Material Structure 28 (2005) pp.1119-1152

[19] Peng B, Pugno N and Espinosa HD (2006) International Journal of Solids and Structures, 43, 3292-3305.

[20] Boroch R, Wiaranowski J, Mueller-Fieldler R, Ebert M and Bagdahn J (2007) Fatigue and Fracture of Engineering Materials and Structures, 30, 2-12

[21] JH Park, CY Kim, SH Choa, CS Lee, WS Che, and JH Song, Key Engineering Materials Vols. 297-300 (2005), pp. 545-550.

[22] JH Park, YJ Kim, MS Myung, CS Lee and SH Choa, NS Choi, Key Engineering Materials Vols. 321-323 (2006), pp. 136-139.

[23] ABAQUS Version 6.4. User's manual. Hibbitt, Karlsson and Sorensen, Inc, RI; 2005.